

GRB 221009A: Spectral signatures based on ALPs candidates

D. Avila Rojas,^{a,1} S. Hernández-Cadena,^a M. M. González,^b A. Pratts,^a R. Alfaro,^a and J. Serna-Franco^a

^aInstituto de Física, Universidad Nacional Autónoma de México, Circuito Exterior, C.U., A. Postal 20-364, 04510 CDMX, México

^bInstituto de Astronomía, Universidad Nacional Autónoma de México, Circuito Exterior, C.U., A. Postal 70-264, 04510 CDMX, México

E-mail: daniel.avila5@ciencias.unam.mx, skerzot@ciencias.unam.mx, magda@astro.unam.mx

Abstract. GRB 221009A has posed a significant challenge to our current understanding of the mechanisms that produce TeV photons in gamma-ray bursts (GRB). On one hand, the Klein-Nishina (KN) effect of the inverse Compton scattering leads to less efficient energy losses of high-energy electrons. In the other hand, at a redshift of 0.151, the TeV spectrum of GRB 221009A undergoes significant absorption by the Extragalactic Background Light (EBL). Therefore, the observation of 18-TeV and 250-TeV photons in this event implies the presence of enormous photon fluxes at the source, which cannot be easily generated by the Synchrotron Self-Compton mechanism in external shocks. As an alternative, some authors have suggested the possibility of converting the TeV-photons into Axion-like particles (ALPs) at the host galaxy, in order to avoid the effects of EBL absorption, and then reconverting them into photons within the Milky Way. While this solution relaxes the requirement of very-high photon fluxes, the KN effect still poses a challenge. Previously, we have showed that the injections of ALPs could explain the observation of 18-TeV photons. Here, we include the energy dependence of the survival probability to determine the spectral conditions that would be required for the injection of such ALPs, limit the ALP's candidate region, and discuss the implications in the maximum particle rate for different light-curve assumptions.

Keywords: gamma-ray burst: general — gamma-ray burst: individual (221009A) — gamma rays: general — emission processes — dark matter — axion-like particles — ALPs

¹Corresponding author.

Contents

1 GRB 221009A observations	1
2 Spectral signatures from ALPs	3
3 Production of ALPs during star collapse	8
4 Final remarks	12

1 GRB 221009A observations

GRB 221009A was first detected on 2022 October 9th by the Fermi-GBM [1] and was followed by several other instruments in many different wavelengths [2–9]. After preliminary analysis of the first observations, T_{90} , fluence and isotropic energy for this event were derived, making this GRB the most luminous ever detected [10, 11]. Spectroscopic observations from GTC’s OSIRIS and the VLT’s X-Shooter were used to estimate the corresponding redshift of $z = 0.151$ [12, 13]. Observations from the Hubble Space Telescope (HST), reveals properties of the host galaxy confirming that the galaxy is prototypical of host galaxies associated with long GRBs. HST observations also shows that this GRB is located near to the center of its host galaxy [14].

There have been fruitless searches for supernova signatures from imaging and spectroscopy studies. However, there is still the possibility that there could be a faint supernova associated [15] to GRB221009A. The James Web Space Telescope analyzed the afterglow emission and found little evidence for variability from early to late times, implying modest contributions from supernova emission. Furthermore, the extreme properties of the burst are likely not linked to an extreme and unusual environment [14].

High energy emission was reported by Fermi-LAT and the Large High Altitude Air Shower Observatory (LHAASO) in the energy range between GeV and TeV. The afterglow temporal profile was fitted from Fermi-LAT data as a power law with an index of 1.32 ± 0.05 [14]. A search for very-high-energy (VHE) photons with no significant detection from this GRB were performed by the High Altitude Water Cherenkov (HAWC) observatory and the High Energy Stereoscopic System (H.E.S.S.) 8 and 53 hours after the trigger, respectively, resulting in upperlimits [16]. In particular, the H.E.S.S. upper limit for energies above 650 GeV rules out the inverse Compton scenario, at least at those times, with the X-ray emission as the synchrotron counterpart. The Fermi Collaboration has recently published their first results for the light curve using data from Fermi-GBM and Fermi-LAT. The total fluence and isotropic energy between 1 – 10,000 keV derived from the individual time intervals from $t_0 - 2.7$ s to $t_0 + 1449.5$ s in the Fermi data are $S = (9.47 \pm 0.07) \times 10^{-2}$ erg cm $^{-2}$ and $E_{\text{iso}} = (1.01 \pm 0.007) \times 10^{55}$ erg, in accordance with other instruments [17, 18].

Fermi-LAT early emission reported a photon with energy of 99.3 GeV at 240 s after GBM trigger [19] and posterior analysis found the highest photon detected by LAT with 397.7 GeV at 33554 s after GBM trigger [20].

One of the highlights from GRB 221009A was the detection of photons with energy from 500 GeV up to 18 TeV from LHAASO within 2000 s since the trigger time at a position

centered at RA = 288.3°, DEC = 19.8° [21]. The relative energy resolution of LHAASO-KM2A is around 36% at 18 TeV, which gives an energy uncertainty of ± 6.48 TeV [22]. This is the very first detection of VHE photons with energies > 10 TeV from a GRB. The detection of at least one 18-TeV photon by LHAASO is not easily explained by the synchrotron-self compton scenario (SSC), which is the most accepted emission model that describes GRBs dynamics. Moreover, attenuation due to interactions with the extragalactic background light (EBL) is expected for photons with energies above 10 TeV, making it more challenging to explain this VHE emission.

Another interesting observation of this GRB is the reported detection by Carpet-2 of a 251-TeV photon 4563 s after GBM's trigger [23]. While certainly intriguing, it is more likely that this photon is associated with a Galactic source as pointed out by the HAWC Collaboration [24]. For this reason, in this paper we only focus on the VHE photons reported by LHAASO.

The origin of the VHE emission has been explored by assuming different scenarios. The most common one is the SSC model, in which VHE gamma-rays are being generated in the external shocks of the GRB jet. It is possible to reach energies up to 1 TeV from the forward shock emission by assuming that the electron spectrum has no energy cutoff [25]. There is also a study using Monte Carlo simulations that predicts a 3.5σ confidence level detection by LHAASO of one 18-TeV photon, but implies the very high value of the differential flux normalization at 0.5 TeV of $\mathcal{O}(10^{-8} - 10^{-7} \text{ TeV}^{-1} \text{ cm}^{-2} \text{ s}^{-1})$, see for example [26], where the differential flux at 500 GeV is $1.14 \times 10^{-10} \text{ TeV}^{-1} \text{ cm}^{-2} \text{ s}^{-1}$. Then, even if the jet structure is assumed to be more complex to reach such energies, such a high value of the differential flux would have profound implications for the energy budget of the event [27, 28]. Therefore, so far, the TeV emission from GRB 221009A is not well described by standard SSC models [29] although other multifrequency detections of the afterglow emission are completely in agreement with SSC.

There have been several searches for neutrinos correlated to GRBs by instruments as IceCube [30–32], Amanda [33, 34] and Antares [35–37] that have resulted in no detections and in strong constraints on the single-zone fireball models of neutrinos and the production of Ultra-high Energy Cosmic Ray (UHECR) during the precursor, prompt and afterglow phases [38]. Despite being considered likely sources of UHECRs due to their large power output, the results of searches for neutrinos correlated with GRBs have been discouraging. As a result, attention has shifted towards other sources, such as active galactic nuclei.

IceCube conducted searches for neutrinos at various time ranges, hours and days from the initial Fermi-GBM trigger, between 800 GeV – 1 PeV. However, no events were found to be coincident with the position of GRB 221009A [39, 40]. Since the non-detection of neutrino emission, the models that forecast the production of neutrinos from GRBs [41] were evaluated by testing the lack of detection. The derived upper limit allowed for the refinement of GRB model parameters [42]. The absence of detection led to a diligent effort to explain this situation through the exploration of various prompt models, as described by [43, 44], and precursor models [45]. Furthermore, novel models that circumvent the EBL attenuation due to heavy neutrinos emerged as a prospective solution [46, 47].

Following the detection of an 18-TeV photon from GRB 221009A, models have been proposed that assume the acceleration of UHECR in this GRB. For instance, UHECR from internal shocks could interact with the EBL and generate photons with energies up to 10 TeV [44]. It has also suggested that UHECR from the reverse shock could also produce 18-TeV photons via synchrotron radiation, assuming an optimistic value of the coefficient $\eta = 1$ in

the proton acceleration timescale [48]. However, for relativistic and ultra-relativistic shocks as expected in GRBs, the coefficient is greater than unity [49]. If a more conservative value of the coefficient ($\eta = 10$) is used, it becomes challenging to detect photons with energies > 10 TeV. Finally, if the GRB is situated at the outer regions of its host galaxy and the Extra-galactic Magnetic Field (EGMF) is as low as $\mathcal{O}(10^{-14}$ G) (to decrease the time delay due to UHCR propagation below 2000 s), photons from the particle cascades of UHECR could explain the LHAASO detection [50].

Some other studies have proposed that the 18-TeV photon detection can be explained by Lorentz Invariance violation effects on $\gamma - \gamma$ absorption [51–53] or non-standard physics such as the existence the Axion Like Particles (ALPs). It was proposed in reference [54] the conversion of TeV-photons into ALPs at the host galaxy to avoid the effects of EBL absorption, followed by reconversion into photons within the Milky Way. In reference [55], a parameter space of ALP candidates was explored to identify those with the highest probability of arriving on Earth as photons. A bound on the Lorentz boost was also obtained. Similarly, reference [56] explored the parameter space of ALPs, but only considering conversions to photons due to the magnetic field of the Milky Way. The authors assumed that the flow of ALPs reaching the Milky Way constitutes one third of the total flux of photons emitted by the GRB. While these solutions relaxes the requirement of very-high photon fluxes, the KN effect still poses a challenge. In a previous publication [57], we considered an initial injection of ALPs and calculated the probability of their arrival on Earth as TeV photons. Our results show a region of allowed parameters of ALPs that could potentially explain the detection of the 18-TeV photon by the LHAASO observatory. However, it was not possible to explain the detection of the 251-TeV photon reported by CARPET-2 using our model. In this paper, we extend our analysis to include the energy dependence of the survival probability of ALPs and the amount of energy carried, in order to determine the spectral conditions that allow for the detection of 18-TeV photons while avoiding the detection of photons with energies greater than 25 TeV (section 2). We calculate the ALPs production during the star collapse through Bremsstrahlung radiation from electrons (section 3) and compare it with the maximum ALP injection rate predicted by our model under various assumptions about the injection time profiles. We discuss the implications of our findings in section 4.

2 Spectral signatures from ALPs

ALPs are hypothetical particles that arise in theories beyond the standard model and are related to the Peccei-Quinn mechanism. This mechanism was proposed to solve the strong CP problem in Quantum Chromodynamics (QCD) and involves the breaking of a symmetry (PQ symmetry) that generates a particle called the Axion. The Lagrangian of ALPs is given by

$$\mathcal{L}_a = \frac{1}{2}(\partial_\mu a \partial^\mu a - m_a^2 a^2) + \frac{1}{4f_a} a F_{\mu\nu} \tilde{F}^{\mu\nu}. \quad (2.1)$$

where a is the ALP field, m_a is the ALP mass, $F_{\mu\nu}$ is the Faraday Tensor and $\tilde{F}^{\mu\nu}$ is its dual. ALPs are of special interest because they are coupled to electromagnetism, which allows for oscillations between photons and ALPs under the influence of source, galactic, and intergalactic magnetic fields. The coupling is expressed as:

$$\mathcal{L}_{a\gamma} = \frac{1}{4f_a} a F_{\mu\nu} \tilde{F}^{\mu\nu} = ag_{a\gamma} \vec{E} \cdot \vec{B}, \quad (2.2)$$

Parameter	Value	Reference
E_{iso}	1.01×10^{55} erg	[17]
d_z	2.23×10^{27} cm	
EBL model	Gilmore	[63]
B_{MW}	$\sim 3\mu\text{G}$	[64]
B_{HG}	$\sim 3\mu\text{G}$	set as MW
d_{HG}	30 kpc	set as MW
d_{MW}	$< 30\text{kpc}$	$\leq d_{\text{MW}}$
α_a	[2.0, 3.0]	set
E_{DM}	0.1, 1, 2, 3%	set

Table 1. Parameters considered in our model. MW, HG stand for Milky Way and Host Galaxy, respectively.

where $g_{a\gamma}$ is the coupling constant and \vec{E} , \vec{B} are the electric and magnetic fields respectively [58]. It is possible for an ALP with a kinetic energy in the TeV range to undergo oscillations and transform into a TeV-photon at any point during its journey towards Earth [59], to survive the attenuation due to the EBL, and reach the TeV detectors. The propagation of the ALP-photon system along the line of sight is described by the propagation equation given by [60].

In this study, we do not make any assumption on an initial population of photons due to their inefficient production by the preferred mechanism, the SSC. Moreover, if TeV photons are produced, their flux must be very high to compensate for the attenuation caused by the EBL. As mentioned section 1, some authors proposed the possibility of photons transforming into ALPs to avoid EBL attenuation, but this scenario would also require a high photon flux, as not all photons would necessarily oscillate into ALPs in the host galaxy or the GRB jet, and not all that do oscillate would convert back to photons in the Milky Way. Therefore, we consider an initial beam consisting solely of ALPs, with the density matrix, $\rho = \Phi\Phi^\dagger$, at $t = 0$ represented as $\rho(0) = \text{diag}(0, 0, 1)$. The probability of survival, $P_{a\gamma}$, resulting from ALPs being detected on Earth as photon is calculated by incorporating all physical parameters, such as those for the medium, magnetic field, electron density, and propagation distance, into the mixing matrix \mathcal{M} . The evolution equation for the density matrix is given by,

$$i\frac{\partial\rho}{\partial l} = [\rho, \mathcal{M}], \quad (2.3)$$

where l is the propagation distance for a given medium. The survival probability is then,

$$P_{a\gamma} = \rho_{1,1}(l) + \rho_{2,2}(l), \quad (2.4)$$

where $\rho_{1,1}$, $\rho_{2,2}$ represent the first and second diagonal elements of the density matrix [61].

We use the open code `gammaALP`, that allow us to calculate the survival probability taking into account different astrophysical environments as Galaxy Host, EBL attenuation, and the Milky Way [62]. Table 1 shows the parameter values used to calculate the survival probability using `gammaALP`.

Previously in [57], we assumed an injection of ALPs with a spectrum that depended solely on the ALP energy, E_a , and was described by a power law function. The values considered for the ALP spectral index, α_a , were 1.8 and 2.5. Here, we introduce a temporal

profile, $\tau(t)$, to the injection while keeping the energy dependency. Then, the ALP spectrum is given by,

$$\Phi_a(E_a, t) = N_o \tau(t) \left(\frac{E_a}{E_{a,0}} \right)^{-\alpha_a}, \quad (2.5)$$

where $E_{a,0} = 1 \text{ TeV}$. We consider different values of the spectral index α_a between 2.0 and 3.0, along with temporal profiles representative of the prompt and afterglow phases. For the prompt phase, we use the light curve published by [65], while for the afterglow phase, we assume a temporal profile that follows a power law $\tau(t) \sim t^{-\beta}$. We choose values of $\beta = 0.5, 1, 2$, which are within the range determined for a sample of 58 long GRBs for the $> 100 \text{ MeV}$ emission by Fermi-LAT [66]. Given a temporal profile, we obtain N_o by considering that the energy carried by the ALPs is a fraction of the total GRB's isotropic energy. Then,

$$\%E_{\text{iso}} = \frac{4\pi d_z}{1+z} N_o \int_{E_{a,\text{min}}}^{E_{a,\text{max}}} \int_{t_{\text{min}}}^{t_{\text{max}}} \tau(t) \left(\frac{E_a}{1 \text{ TeV}} \right)^{-\alpha_a+1} dt dE_a, \quad (2.6)$$

where d_z is the luminosity distance to the source, z is the redshift, t_{min} and t_{max} define the time interval when the ALP injection occurs, and $E_{a,\text{min}}$ and $E_{a,\text{max}}$ are the maximum and minimum energies of the injected ALPs. We consider that the total energy carried by the ALPs could represent from 0.1 up to 30% of E_{iso} . Finally, the number of observed photons by LHAASO, N_γ , is obtained by considering the effective area $A(E_\gamma)$ of LHAASO-KM2A as function of the photon energy (E_γ), the normalization (N_o) of the ALPs spectrum, and the survival probability, $P_{a\gamma}(E_\gamma)$, and is given as,

$$N_\gamma = \int_{E_{\gamma,\text{min}}}^{E_{\gamma,\text{max}}} \int_{t_0}^{t_{2000}} \Phi_\gamma(E_\gamma) A(E_\gamma) dt dE_\gamma \quad (2.7)$$

$$= N_o \int_{E_{\gamma,\text{min}}}^{E_{\gamma,\text{max}}} \int_{t_0}^{t_{2000}} \Phi_a(E_a, t) P_{a\gamma}(E_\gamma) A(E_\gamma) dt dE_\gamma \quad (2.8)$$

$$= N_o \int_{E_{\gamma,\text{min}}}^{E_{\gamma,\text{max}}} \int_{t_0}^{t_{2000}} \tau(t) \left(\frac{E_a}{1 \text{ TeV}} \right)^{-\alpha_a} P_{a\gamma}(E_\gamma) A(E_\gamma) dt dE_\gamma. \quad (2.9)$$

Equation 2.9 is solved considering equation 2.6, that the injection of ALPs last as long as the photon observation (2000 s as reported by LHAASO) and, that $E_a \sim E_\gamma$ since the mass of the ALP is much smaller than its kinetic energy. Note that the total number of detected photons does not depend on the time profile of the ALP injection, although the normalization factor N_o does. The values of m_a and $g_{a\gamma}$ are taken from 10^{-5} to 10^{-8} eV and from 3.16×10^{-12} to $10^{-10} \text{ GeV}^{-1}$, respectively.

Then, we impose the following conditions on the number of observed photons:

1. At least 0.5 photons with energies between 10 – 25 TeV.
2. Less than 0.5 photons with energies $> 25 \text{ TeV}$.

These conditions were set based on the fact that the highest-energy photon detected by LHAASO had an energy of 18 TeV, and no detection has been reported beyond the energy uncertainty band at this energy ($\pm 6.48 \text{ TeV}$). We show the allowed parameter space for

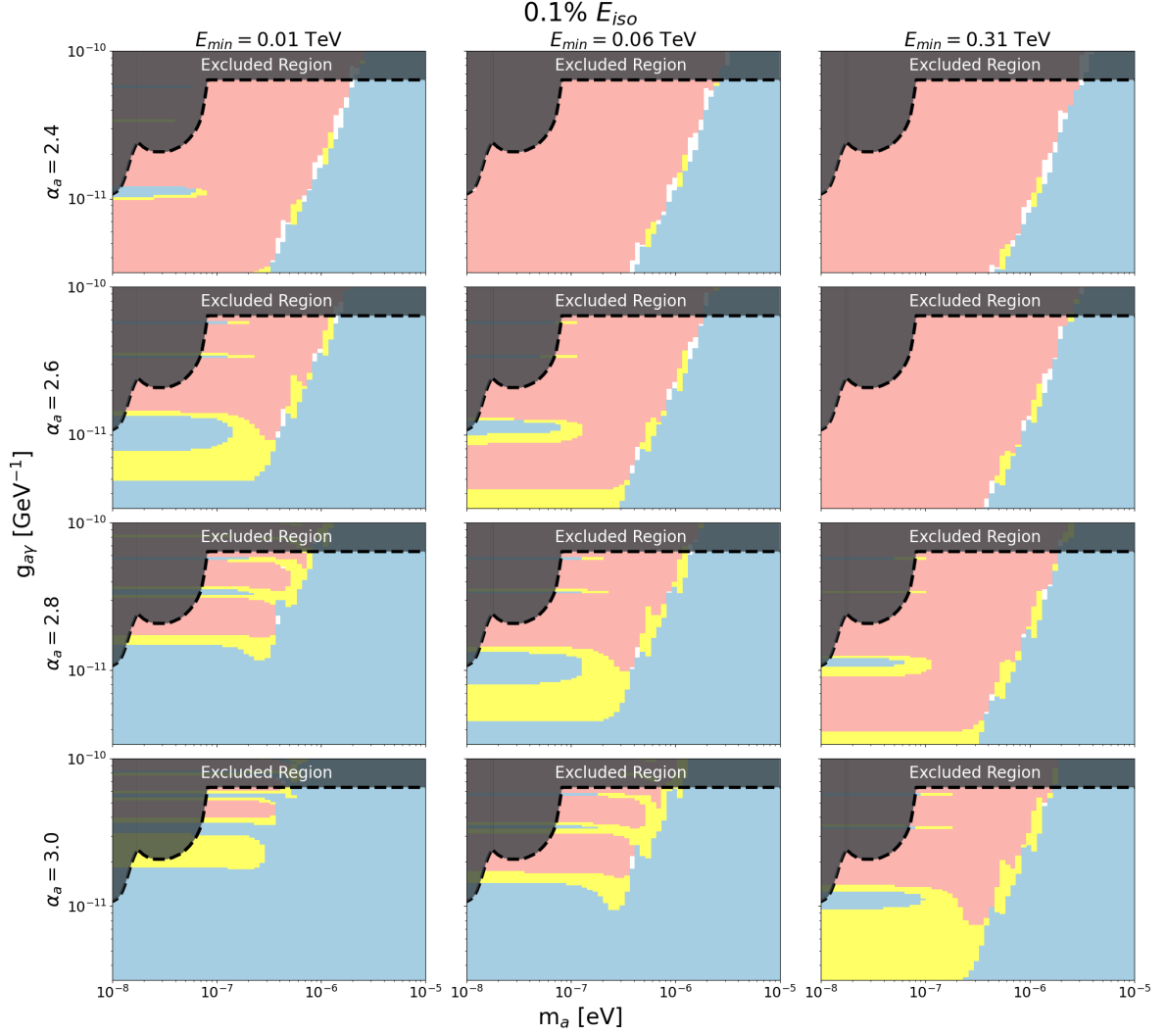


Figure 1. ALPs parameter space taking different values of E_{\min} and α_a for 0.1% of the E_{iso} taken by the ALPs burst. Pink: region with > 0.5 photons in the energy range 10 – 25 TeV. Blues: region with < 0.5 photons for energies above 25 TeV. Yellow: Allowed region obtained from the intersection of the pink and blue regions.

($\%E_{\text{iso}} = 0.1$ and, different values of α_a and E_{\min} in figure 1). Interestingly, it is not possible to find ALP candidates when the spectra is harder than -2.4 or when the minimum energy of the injected ALPs is above 1 TeV. Furthermore, as seen in figures 2 and 3, as the amount of energy carried by the ALPs increases, a softer spectra and a lower E_{\min} (tens of GeV or lower) are required. It is interesting to note that if an injected beam of ALPs by the GRB progenitor is responsible for the observed photons at 18 TeV, their spectra must be soft, with most of the energy being carried by ALPs with energies much lower than the observed photons (tens or hundreds of GeV), and the total energy carried by ALPs must be a few percent of E_{iso} .

To determine whether the allowed ALP candidates can reproduce the observed photon flux, we calculate the survival probability for each candidate and fit the resulting photon

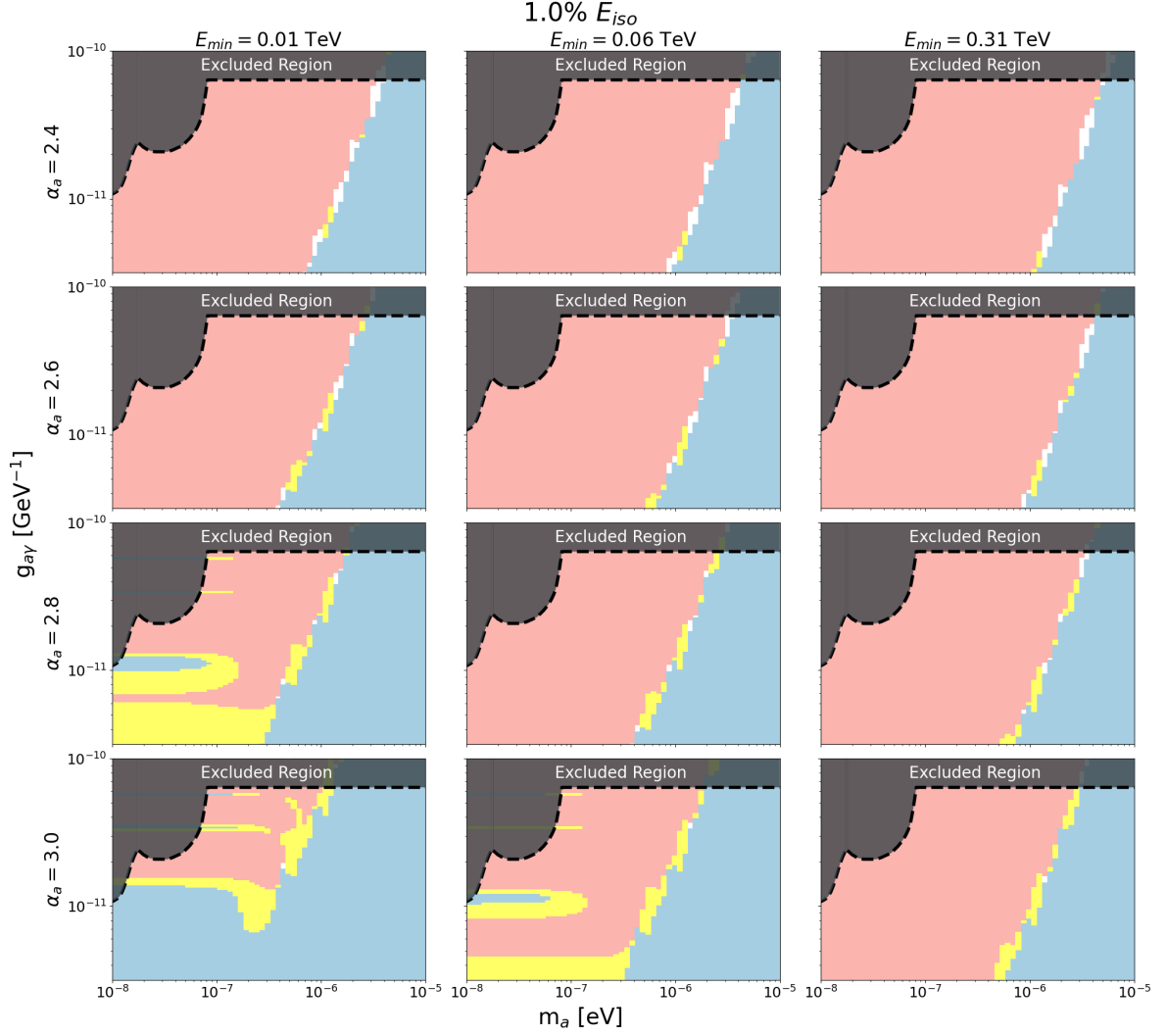


Figure 2. ALPs parameter space taking different values of E_{\min} and α_a for 1% of the E_{iso} taken by the ALPs burst. The color code is the same as in Figure 1.

spectrum that reaches Earth. Figure 4 shows the survival probability as well as the fitted observed photon spectrum for the candidate defined by $g_{a\gamma} = 1.75 \times 10^{-11} \text{GeV}^{-1}$, $m_a = 5.46 \times 10^{-7} \text{eV}$ with $\%E_{\text{iso}} = 0.1$, $E_{\min} = 31 \text{ GeV}$, and $\alpha_a = 3.0$. For this candidate, the survival probability increases with energy, and a soft ALP spectrum is required to avoid observing photons beyond energies greater than 25 TeV. The resulting photon flux is characterized by a hard photon index of -2.15. We repeated this analysis for every permitted ALP candidate and show the resulting photon index and number of observed photons by LHAASO with energies larger than 500 GeV in Figure 5. We considered $\%E_{\text{iso}}$ values of 0.1, 1, and 3 percent, $E_{\min} = 31$, and $\alpha_a = 3.0$. We found that observed ALP candidates that reproduce hard photon spectra can be responsible for only a few tens of photons with energies larger than 500 GeV. Therefore, to explain a large flux of photons with $E > 500 \text{ GeV}$, the observed photon flux must be soft. Nevertheless, an injection of ALPs by the progenitor can still contribute up to a tenth of the photons observed by LHAASO with energies larger than 500

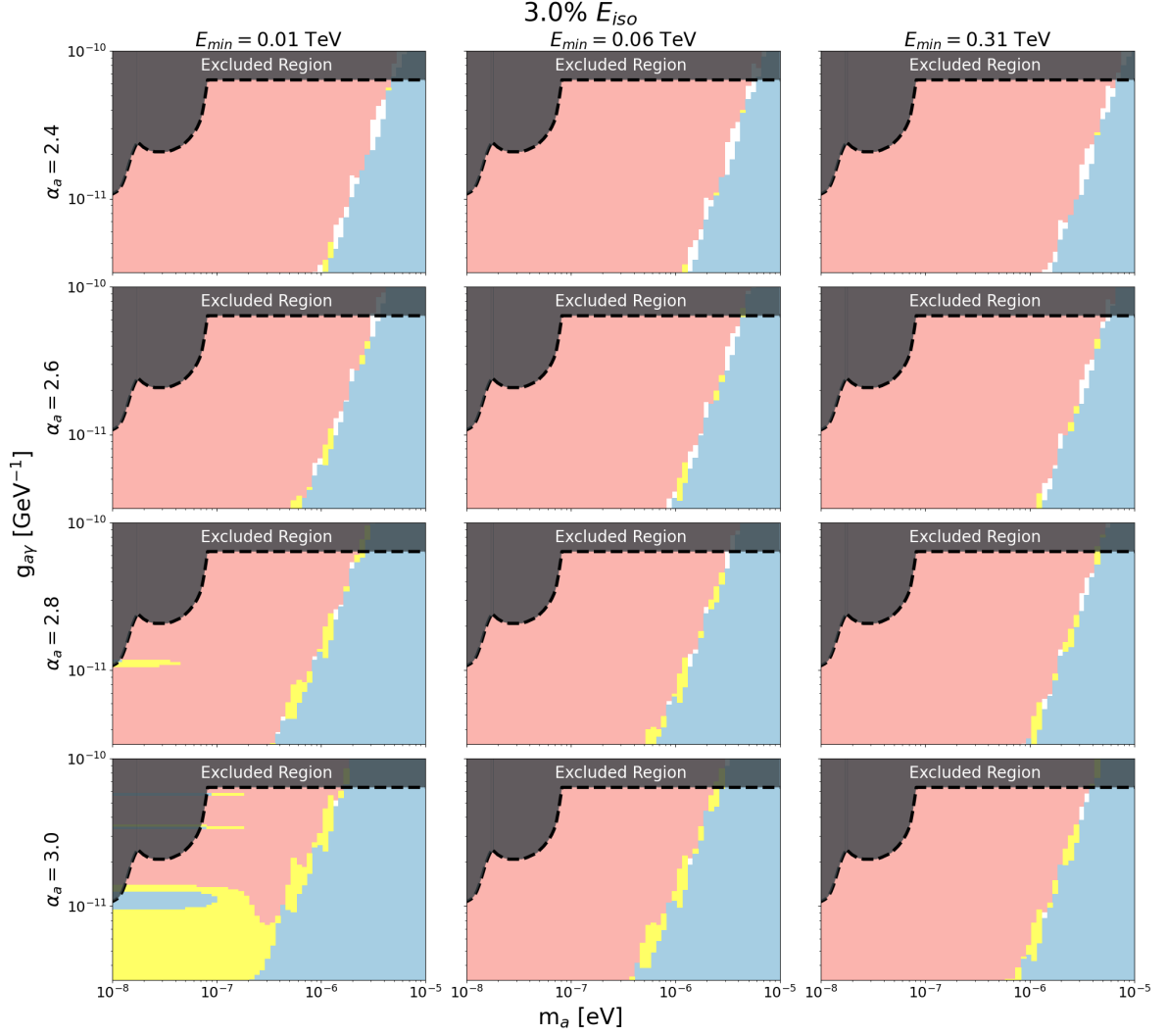


Figure 3. ALPs parameter space taking different values of E_{\min} and α_a for 3% of the E_{iso} taken by the ALPs burst. The color code is the same as in Figure 1.

GeV.

3 Production of ALPs during star collapse

The GRB 221009A is classified as a long GRB [1, 2], and the most likely progenitor is the collapse of a massive star [67, 68]. When a star burns all of its fuel and reaches iron in its core, the core can no longer sustain the gravitational force, and it undergoes a collapse. The collapse is stopped by the degeneracy pressure of the different particles inside the core, resulting in temperatures on the order of MeV and densities several times that of the nuclear density. At some point, the degeneracy of nucleons can stop the collapse, and a shock wave propagates outwards while more material from the outer layers of the star continues to fall onto the core. The compact object in this phase is called a protoneutron star (PNS), and during the bounce generated by the shock wave, neutrinos are produced. The production of

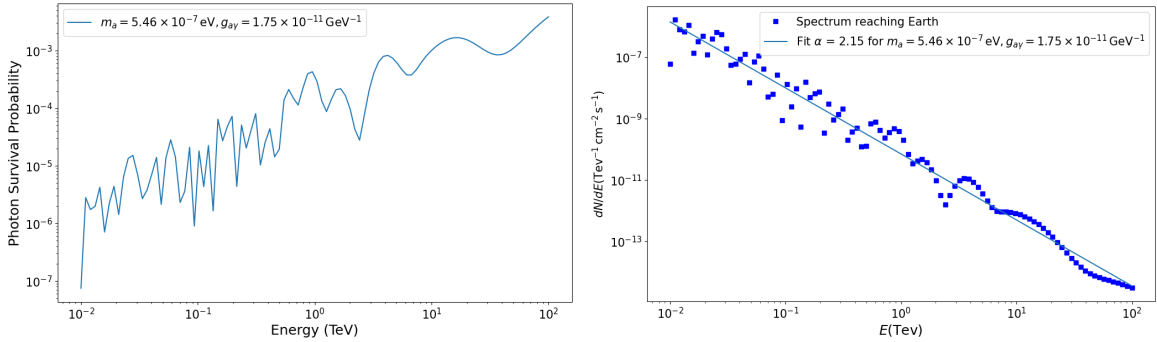


Figure 4. Left: Survival probability for a candidate to reach Earth as a photon. The value of the parameters for this ALP candidate are: $m_a = 5.46 \times 10^{-7}$ eV and $g_{a\gamma} = 1.75 \times 10^{-11}$ GeV $^{-1}$. Right: Fitted photon spectrum for the candidate as in the left plot.

axions and ALPs, which are hypothetical particles beyond the Standard Model, can also be possible during this process.

Previous studies have investigated the production of axions to set constraints on the coupling constants of axions and electrons, using the observations of SN 1987A [69–71]. Other works have explored the contributions of different species of particles, such as protons and pions, to the production of axions and ALPs in the PNS [72–74].

The literature contains various simulations that aim to understand the temporal evolution of dynamic and environmental conditions inside the PNS [73]. However, the numerical density of protons, temperature, and chemical potential inside the PNS are not fully comprehended, and there are several challenges in fully understanding the mechanisms and processes that lead to the explosion and creation of a GRB. Nonetheless, we can use these time profiles to estimate the production rate of ALPs and their contribution to the photon flux emitted by the GRB. One of the dominant processes contributing to ALP production for masses below tens of MeV is Bremsstrahlung-like radiation, which occurs at all radii inside the PNS and can last up to 10 s [70]. The total ALP production rate due to Bremsstrahlung is a result of the contributions from electron, pion, and proton collisions with the effective number of protons n_p^{eff} present in the PNS. However, in this work, we only consider the contribution from electron Bremsstrahlung, as the contribution from the other particles has been found to be of the same order of magnitude as that of electrons [73].

We follow the methodology presented in [70, 72] to obtain the rate of ALPs production per unit time per unit of energy, denoted as $dn_{\text{ALP}}/dt dE$ and given as,

$$\frac{dn_a}{dt dE} = \frac{1}{64\pi^6} \int_{-1}^1 d\cos\theta_{ia} \int_{-1}^1 d\cos\theta_{if} \int_0^{2\pi} d\delta \int_{m_e}^{\infty} dE_f p_i p_f p_a |\mathcal{M}|^2 f_i (1 - f_f), \quad (3.1)$$

where p_i , p_f are the norm of the initial and final spatial momentum of the electron, and p_a is the norm of the spatial momentum of the ALP radiated. The term of $|\mathcal{M}|^2$ is the spin-average mixing matrix element for the Bremsstrahlung process. We use the expression for $|\mathcal{M}|^2$ given by [72]. The function f describes the Fermi-Dirac distribution of electrons, and the subscripts i and f correspond to the initial and final states of the electron. The term $1 - f_f$ is the Pauli block term. The integral is computed over the energy of the outgoing electron, E_f , the angles between the initial electron momentum and the ALP momentum θ_{ia} ,

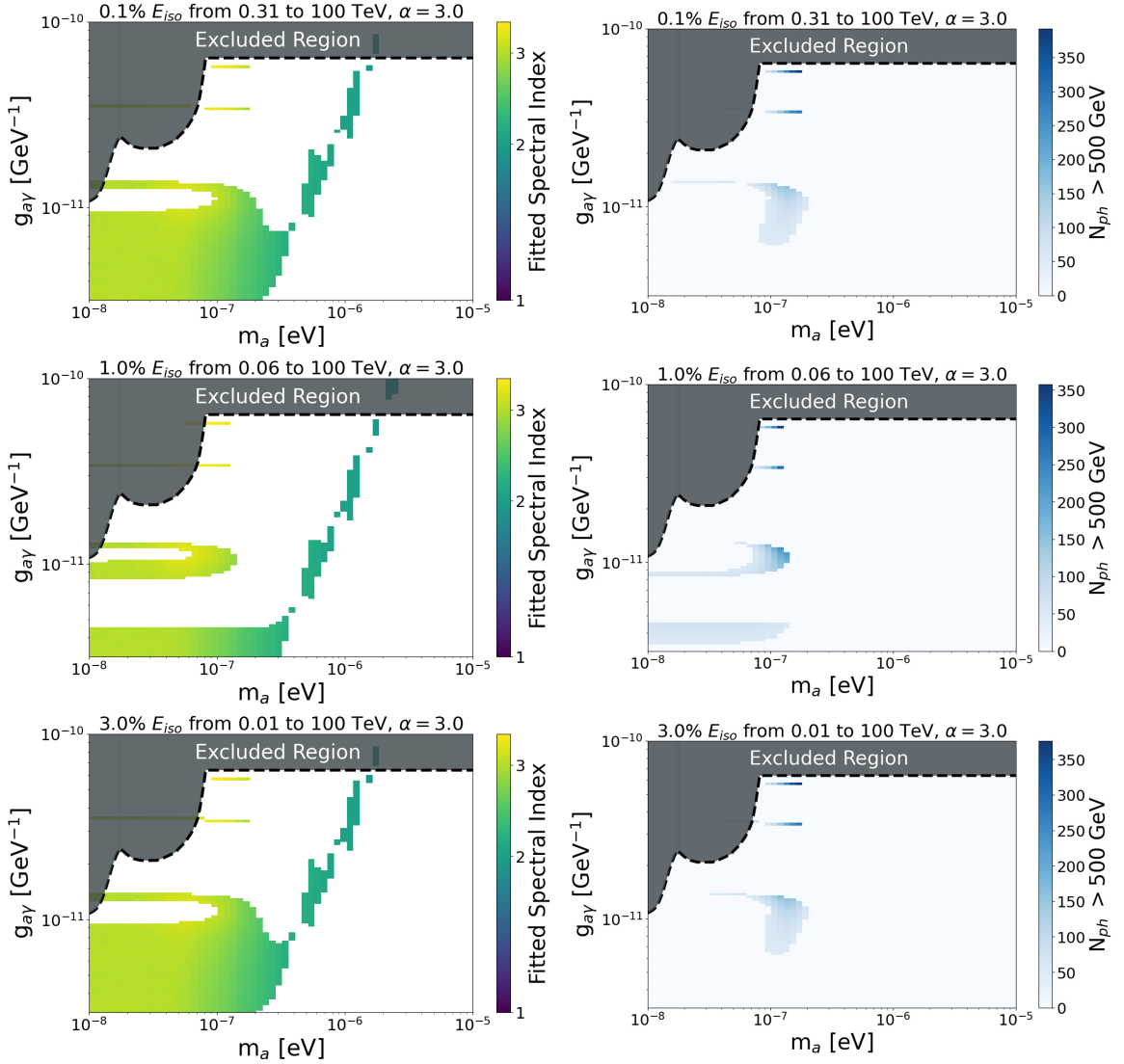


Figure 5. Left row: Fitted spectral indexes of the photon flux from candidates in the permitted region. Right row: Number of photons > 500 GeV for ALPs candidates in the permitted region satisfying the condition $N_{ph} > 50$ photons. Plots show results for different values of $\%E_{iso}$ taken for the ALPs production, the ALPs flux spectral index α_a and E_{min} .

and the final electron momentum, θ_{if} ; and the angle δ between the planes determined by the momentum vectors $\vec{p}_i - \vec{p}_a$ and $\vec{p}_i - \vec{p}_f$.

Additional parameters and their radial and temporal profiles associated with the PNS need to be considered to obtain the production rate of ALPs in the PNS after the bounce. They depend on the different simulations of the PNS. Examples of the temporal and radial profiles can be found in [70, 73]. Here, we only use representative values for the different quantities. Table 2 shows the values we used to compute dn_{ALP}/dtE . For the radial profile, we assume that the quantities are constants within a radial annulus of 5 km centered around the radius where the temperature is maximum (~ 10 km). This is a conservative approximation based on the radial profile shown in figure 4 of reference [73]). For the temporal profiles, we only compute the production of ALPs during the first second after bounce.

Quantity	Symbol	Value
Temperature	T	50 MeV
e -Chemical potential	μ_e	200 MeV
Effective proton density	n_p^{eff}	10^{37} cm^{-3}

Table 2. Values of PNS variables used to compute the ALP-production rate.

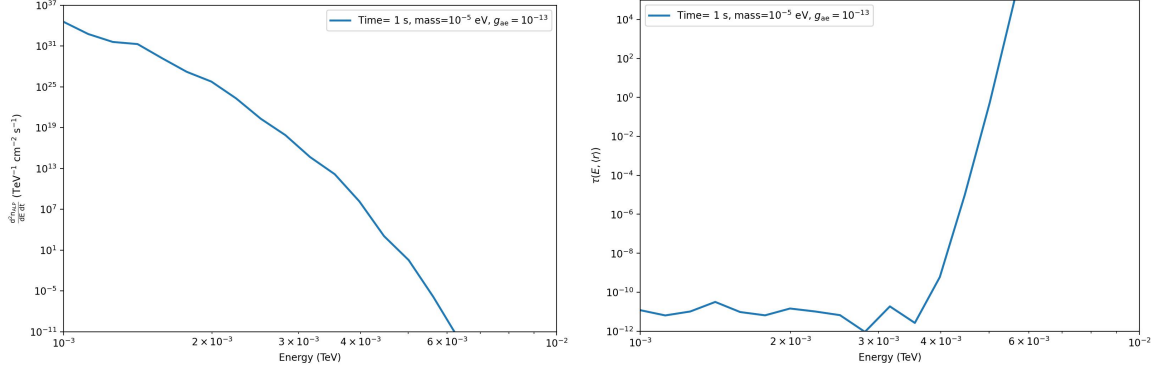


Figure 6. Production rate and optical depth for ALPs inside the PNS. **Left.** Production rate of ALPs assuming that ALPs are produced by bremsstrahlung of electrons with protons in the PNS. We observe that the spectra has a hard cutoff in the ALP energy and particles with energies above 6 GeV are not produced. **Right.** Optical depth $\tau(E_{\text{ALP}}, \langle r \rangle)$ as a function of the energy of the ALP. $\tau(E_{\text{ALP}}, \langle r \rangle)$, increase exponentially for energies above ~ 3 GeV, and ALPs with energies above this threshold are reabsorbed quickly inside the PNS and cannot escape from the PNS.

We restrict the energy range of the outgoing electron to 1 MeV – 1 TeV as this interval contributes the most to the production of ALPs, and limit the calculation of the ALP-production rate to the energy interval between 1 GeV and 10 GeV as we are interested in comparing the number of ALPs produced in the PNS with the maximum photon flux when different temporal profiles are considered, see section 2.

Additionally, we estimate the optical depth $\tau(E_{\text{ALP}}, \langle r \rangle)$ of the medium by computing the inverse of the mean free path for the ALP-Bremsstrahlung process, λ_{B}^{-1} . We use the following expression to compute λ_{B}^{-1} [70]:

$$\lambda_{\text{B}}^{-1} = \frac{\exp(E_{\text{ALP}}/T) - 1}{32\pi^4} \times \int_{-1}^1 d \cos \theta_{\text{ia}} \int_{-1}^1 d \cos \theta_{\text{if}} \int_0^{2\pi} d\delta \int_{m_e}^{\infty} dE_{\text{f}} \frac{p_{\text{i}} p_{\text{f}}}{p_{\text{ALP}}} |\mathcal{M}|^2 f_{\text{ALP+f}} (1 - f_{\text{f}}), \quad (3.2)$$

then, we compute $\tau(E_{\text{ALP}}, \langle r \rangle)$ as:

$$\tau(E, \langle r \rangle) = \frac{\Delta r}{\lambda_{\text{B}}^{-1}} \quad (3.3)$$

where, as in the case for the production rate of ALPs, we assume that the PNS variables are constant within a radius where the temperature T reaches its maximum, so we only need to multiply by the width of the annular ring, Δr , where the ALPs are produced.

Figure 6 shows the production rate (left) and the optical depth $\tau(E_{\text{ALP}}, \langle r \rangle)$ (right) of ALPs produced by Bremsstrahlung of electrons with protons inside the PNS. For the

Maximum Normalization [$\text{TeV}^{-1} \text{cm}^{-2} \text{s}^{-1}$]			
at E (MeV)	15	500	1000
Prompt Profile	4×10^{-4}	1×10^{-8}	2×10^{-9}
Afterglow Profile $\sim t^{-0.5}$	2×10^{-4}	5×10^{-9}	6×10^{-10}
Afterglow Profile $\sim t^{-1}$	2×10^{-3}	4×10^{-8}	5×10^{-9}
Afterglow Profile $\sim t^{-2}$	7×10^{-3}	2×10^{-7}	2×10^{-8}

Table 3. Maximum ALP differential flux for different temporal profiles at 15, 500 and 1000 GeV for a burst of ALPs carrying 0.1% of the isotropic energy integrated from 0.01 – 100 TeV. This was calculated for an ALPs spectrum of $\alpha_a = 3.0$.

calculation, we assume that the ALP has a mass of 10^{-5} eV and a constant coupling with electrons g_{ae} of 10^{-13} . The value of g_{ae} is consistent with the bounds obtained by CAST and the constraint obtained from cooling of white dwarfs and low-mass red giants to the parameter space of $g_{a\gamma} - g_{ae}$ [75]. We observe that the number of ALPs produced has an energy cutoff, and ALPs with energies above several GeV cannot be produced by this process. Moreover, the optical depth $\tau(E, \langle r \rangle)$ indicates that ALPs with energies in the GeV scale are quickly reabsorbed by the environment inside the PNS and are trapped inside the PNS.

Finally, we calculate the maximum differential flux of ALPs at energies of 15, 500, and 1000 GeV using the temporal profiles mentioned in Section 2 (see Table 3). Comparing these values with those in Figure 6, it is clear that the production of ALPs during the star collapse by electron Bremsstrahlung cannot account for the photons that would be produced with energies in the GeV range if the observed photon at 18 TeV is explained by an injection of ALPs by the progenitor. Thus, other production mechanisms of ALPs must be studied.

4 Final remarks

We have analyzed the allowed parameter space for an ALPs burst released at the GRB that could potentially explain the detection of the 18, TeV photon by LHAASO. To narrow down the candidates, we set the condition that the number of photons between 10 – 25, TeV must be at least 0.5 photons, while the number of photons above 25, TeV must be less than 0.5 photons. Based on this, the permitted regions are more favorable if the ALPs carry just a fraction of the GRB energy, which is less than 3%. Moreover, the energy must be carried by ALPs with energy as low as tens of GeV through a soft spectrum extending at least up to tens of TeV.

We calculated the resulting gamma-ray spectrum of the candidates in the permitted regions, and the fitted spectral indexes ranged between 1.8 – 3.0, which are comparable with the ones reported between energies of 100, MeV – 500, GeV by [76]. Then, we calculated the number of photons $> 500, \text{GeV}$ for the candidates contained in the permitted regions and found that it does not exceed 400 photons. This means that the contribution to the photon flux from ALPs above this energy could be up to 7% of the photons reported by LHAASO. This is consistent with previous studies [77] of GRB emission at hundred of GeV and up to 4 TeV where the Synchrotron self-Compton mechanisms describes the observations reasonably well. While the mechanisms of production and acceleration of light DM particles such as ALPs are still under investigation, a population of ALPs in the studied region would be able to explain the 18-TeV photon and a fraction of the photons above 500, GeV

We also investigated the possibility of ALP production from a collapsing massive star as the mechanism responsible for the observed 18-TeV photon at GRB 221009A. We computed the ALP production rate via Bremsstrahlung of electrons with protons inside the PNS, but the resulting ALPs did not have the required energies or particle rate production to explain the observed photon by LHAASO. Other particles in the PNS could be considered, such as protons, neutrons, and pions, but their contributions do not change our conclusions. Other ALP production mechanisms have been proposed in previous studies, such as via first-order phase transition [78], but these are limited by the conditions inside the PNS and the high densities in its inner regions, which prevent ALPs with energies above GeV from escaping. Therefore, our result may indicate that ALPs would need to be produced in external regions to the PNS. In other words, the ALPs needed to explain the 18-TeV photon must be produced through other mechanisms that do not depend on the thermal properties of the PNS, or they must be accelerated to GeV and TeV energies by an unknown mechanism.

Acknowledgments

This work was supported by UNAM-PAPIIT project number IG101323.

References

- [1] P. Veres, E. Burns, E. Bissaldi, S. Lesage, O. Roberts and Fermi GBM Team, *GRB 221009A: Fermi GBM detection of an extraordinarily bright GRB*, *GRB Coordinates Network* **32636** (2022) 1.
- [2] S. Dichiara, J.D. Gropp, J.A. Kennea, N.P.M. Kuin, A.Y. Lien, F.E. Marshall et al., *Swift J1913.1+1946 a new bright hard X-ray and optical transient*, *GRB Coordinates Network* **32632** (2022) 1.
- [3] A. Tiengo, F. Pintore, S. Mereghetti, R. Salvaterra and a larger Collaboration, *Swift/XRT discovery of multiple dust-scattering X-ray rings around GRB 221009A*, *GRB Coordinates Network* **32680** (2022) 1.
- [4] K. Pellegrin, K. Rumstay and D. Hartmann, *GRB 221009A: SARA-RM 1m Optical Afterglow Detection*, *GRB Coordinates Network* **32852** (2022) 1.
- [5] Y.D. Hu, V. Casanova, E. Fernandez-Garcia, M.A. Castro Tirado, M.D. Caballero-Garcia, I. Olivares et al., *GRB 221009A BOOTES-2/TELMA and OSN optical detections*, *GRB Coordinates Network* **32644** (2022) 1.
- [6] W. Farah, J. Bright, A. Pollak, A. Siemion, D. DeBoer, R. Fender et al., *GRB221009A/Swift J1913.1+1946: ATA follow-up observations*, *GRB Coordinates Network* **32655** (2022) 1.
- [7] Y. Liu, C. Zhang, Z.X. Ling, H.Q. Cheng, C.Z. Cui, D.W. Fan et al., *GRB 221009A: LEIA X-ray Afterglow Detection*, *GRB Coordinates Network* **32767** (2022) 1.
- [8] J.M. Durbak, A.S. Kutyrev, I. Andreoni, K. De, E. Troja, S.B. Cenko et al., *GRB 221009A or Swift J1913.1+1946: PRIME near-infrared detection*, *GRB Coordinates Network* **32654** (2022) 1.
- [9] R. Brivio, M. Ferro, P. D’Avanzo, D. Fugazza, A. Melandri, S. Covino et al., *GRB 221009A: REM optical and NIR detection of the afterglow*, *GRB Coordinates Network* **32652** (2022) 1.
- [10] S. Lesage, P. Veres, O.J. Roberts, E. Burns, E. Bissaldi and Fermi GBM Team, *GRB 221009A: Fermi GBM observation*, *GRB Coordinates Network* **32642** (2022) 1.
- [11] Z.L. Tu and F.Y. Wang, *The Correlation between Isotropic Energy and Duration of Gamma-Ray Bursts*, *ApJ* **869** (2018) L23 [[1811.12561](https://arxiv.org/abs/1811.12561)].

- [12] A.J. Castro-Tirado, R. Sanchez-Ramirez, Y.D. Hu, M.D. Caballero-Garcia, M.A. Castro Tirado, E. Fernandez-Garcia et al., *GRB 221009A: 10.4m GTC spectroscopic redshift confirmation*, *GRB Coordinates Network* **32686** (2022) 1.
- [13] A. de Ugarte Postigo, L. Izzo, G. Pugliese, D. Xu, B. Schneider, J.P.U. Fynbo et al., *GRB 221009A: Redshift from X-shooter/VLT*, *GRB Coordinates Network* **32648** (2022) 1.
- [14] A.J. Levan, G.P. Lamb, B. Schneider, J. Hjorth, T. Zafar, A. de Ugarte Postigo et al., *The first just spectrum of a grb afterglow: No bright supernova in observations of the brightest grb of all time, grb 221009a*, *The Astrophysical Journal Letters* **946** (2023) L28.
- [15] M. Shrestha, D.J. Sand, K.D. Alexander, K.A. Bostroem, G. Hosseinzadeh, J. Pearson et al., *Limit on Supernova Emission in the Brightest Gamma-Ray Burst, GRB 221009A*, *ApJ* **946** (2023) L25 [2302.03829].
- [16] F. Aharonian, F.A. Benkhali, J. Aschersleben, H. Ashkar, M. Backes, A. Baktash et al., *H.E.S.S. Follow-up Observations of GRB 221009A*, *ApJ* **946** (2023) L27 [2303.10558].
- [17] S. Lesage, P. Veres, M.S. Briggs, A. Goldstein, D. Kocevski, E. Burns et al., *Fermi-GBM Discovery of GRB 221009A: An Extraordinarily Bright GRB from Onset to Afterglow*, *arXiv e-prints* (2023) arXiv:2303.14172 [2303.14172].
- [18] J. Yang, X.-H. Zhao, Z. Yan, X.I. Wang, Y.-Q. Zhang, Z.-H. An et al., *Synchrotron Radiation Dominates the Extremely Bright GRB 221009A*, *arXiv e-prints* (2023) arXiv:2303.00898 [2303.00898].
- [19] R. Pilleri, E. Bissaldi, N. Omodei, G. La Mura, F. Longo and Fermi-LAT team, *GRB 221009A: Fermi-LAT refined analysis*, *GRB Coordinates Network* **32658** (2022) 1.
- [20] Z.-Q. Xia, Y. Wang, Q. Yuan and Y.-Z. Fan, *GRB 221009A: a 397.7 GeV photon observed by Fermi-LAT at 0.4 day after the GBM trigger*, *GRB Coordinates Network* **32748** (2022) 1.
- [21] Y. Huang, S. Hu, S. Chen, M. Zha, C. Liu, Z. Yao et al., *LHAASO observed GRB 221009A with more than 5000 VHE photons up to around 18 TeV*, *GRB Coordinates Network* **32677** (2022) 1.
- [22] X.-H. Ma, Y.-J. Bi, Z. Cao, M.-J. Chen, S.-Z. Chen, Y.-D. Cheng et al., *Chapter 1 lhaaso instruments and detector technology **, *Chinese Physics C* **46** (2022) 030001.
- [23] D.D. Dzhappuev, Y.Z. Afashokov, I.M. Dzaparova, T.A. Dzhatdov, E.A. Gorbacheva, I.S. Karpikov et al., *Swift J1913.1+1946/GRB 221009A: detection of a 250-TeV photon-like air shower by Carpet-2*, *The Astronomer's Telegram* **15669** (2022) 1.
- [24] N. Fraija, M. Gonzalez and HAWC Collaboration, *Swift J1913.1+1946/GRB 221009A: Galactic sources of > 100 TeV-photon in spatial coincidence with the 250-TeV photon-like air shower reported by Carpet-2*, *The Astronomer's Telegram* **15675** (2022) 1.
- [25] T. Laskar, K.D. Alexander, R. Margutti, T. Eftekhari, R. Chornock, E. Berger et al., *The Radio to GeV Afterglow of GRB 221009A*, *ApJ* **946** (2023) L23 [2302.04388].
- [26] H. Abdalla, R. Adam, F. Aharonian, F. Ait Benkhali, E.O. Angüner, M. Arakawa et al., *A very-high-energy component deep in the γ -ray burst afterglow*, *Nature* **575** (2019) 464 [1911.08961].
- [27] M.A. Williams, J.A. Kennea, S. Dichiara, K. Kobayashi, W.B. Iwakiri, A.P. Beardmore et al., *GRB 221009A: Discovery of an Exceptionally Rare Nearby and Energetic Gamma-Ray Burst*, *ApJ* **946** (2023) L24.
- [28] Y. Sato, K. Murase, Y. Ohira and R. Yamazaki, *Two-component jet model for multi-wavelength afterglow emission of the extremely energetic burst GRB 221009A*, *MNRAS* (2023) [2212.09266].

- [29] D.A. Kann, S. Agayeva, V. Aivazyan, S. Alishov, C.M. Andrade, S. Antier et al., *GRANDMA and HXMT Observations of GRB 221009A – the Standard-Luminosity Afterglow of a Hyper-Luminous Gamma-Ray Burst*, *arXiv e-prints* (2023) arXiv:2302.06225 [2302.06225].
- [30] M.G. Aartsen, M. Ackermann, J. Adams, J.A. Aguilar, M. Ahlers, M. Ahrens et al., *Extending the Search for Muon Neutrinos Coincident with Gamma-Ray Bursts in IceCube Data*, *ApJ* **843** (2017) 112 [1702.06868].
- [31] R. Abbasi, M. Ackermann, J. Adams, J.A. Aguilar, M. Ahlers, M. Ahrens et al., *Follow-up of Astrophysical Transients in Real Time with the IceCube Neutrino Observatory*, *ApJ* **910** (2021) 4 [2012.04577].
- [32] R. Abbasi, M. Ackermann, J. Adams, J.A. Aguilar, M. Ahlers, M. Ahrens et al., *Searches for Neutrinos from Gamma-Ray Bursts Using the IceCube Neutrino Observatory*, *ApJ* **939** (2022) 116 [2205.11410].
- [33] A. Achterberg, M. Ackermann, J. Adams, J. Ahrens, K. Andeen, J. Auffenberg et al., *Search for Neutrino-induced Cascades from Gamma-Ray Bursts with AMANDA*, *ApJ* **664** (2007) 397 [astro-ph/0702265].
- [34] A. Achterberg, M. Ackermann, J. Adams, J. Ahrens, K. Andeen, J. Auffenberg et al., *The Search for Muon Neutrinos from Northern Hemisphere Gamma-Ray Bursts with AMANDA*, *ApJ* **674** (2008) 357 [0705.1186].
- [35] A. Albert, M. André, M. Anghinolfi, G. Anton, M. Ardid, J.J. Aubert et al., *Search for high-energy neutrinos from bright GRBs with ANTARES*, *MNRAS* **469** (2017) 906 [1612.08589].
- [36] A. Albert, M. André, M. Anghinolfi, G. Anton, M. Ardid, J.J. Aubert et al., *Constraining the contribution of Gamma-Ray Bursts to the high-energy diffuse neutrino flux with 10 yr of ANTARES data*, *MNRAS* **500** (2021) 5614 [2008.02127].
- [37] ANTARES Collaboration, A. Albert, M. André, M. Anghinolfi, G. Anton, M. Ardid et al., *ANTARES upper limits on the multi-TeV neutrino emission from the GRBs detected by IACTs*, *J. Cosmology Astropart. Phys.* **2021** (2021) 092 [2011.11411].
- [38] F. Lucarelli, G. Oganessian, T. Montaruli, M. Branchesi, A. Mei, S. Ronchini et al., *Neutrino search from γ -ray bursts during the prompt and X-ray afterglow phases using 10 years of IceCube public data*, *A&A* **672** (2023) A102 [2208.13792].
- [39] IceCube Collaboration, *GRB 221009A: Upper limits from a neutrino search with IceCube, GRB Coordinates Network* **32665** (2022) 1.
- [40] R. Abbasi, M. Ackermann, J. Adams, S.K. Agarwalla, N. Aggarwal, J.A. Aguilar et al., *Limits on Neutrino Emission from GRB 221009A from MeV to PeV Using the IceCube Neutrino Observatory*, *ApJ* **946** (2023) L26 [2302.05459].
- [41] S.S. Kimura, *Neutrinos from Gamma-ray Bursts*, *arXiv e-prints* (2022) arXiv:2202.06480 [2202.06480].
- [42] K. Murase, M. Mukhopadhyay, A. Kheirandish, S.S. Kimura and K. Fang, *Neutrinos from the Brightest Gamma-Ray Burst?*, *ApJ* **941** (2022) L10 [2210.15625].
- [43] S. Ai and H. Gao, *Model Constraints Based on the IceCube Neutrino Nondetection of GRB 221009A*, *ApJ* **944** (2023) 115 [2210.14116].
- [44] A. Rudolph, M. Petropoulou, W. Winter and Ž. Bošnjak, *Multi-messenger Model for the Prompt Emission from GRB 221009A*, *ApJ* **944** (2023) L34 [2212.00766].
- [45] M. Bhattacharya, J.A. Carpio, K. Murase and S. Horiuchi, *High-energy neutrino emission from magnetized jets of rapidly rotating protomagnetars*, *MNRAS* **521** (2023) 2391 [2210.08029].

- [46] K. Cheung, *The Role of a Heavy Neutrino in the Gamma-Ray Burst GRB-221009A*, *arXiv e-prints* (2022) arXiv:2210.14178 [2210.14178].
- [47] A.Y. Smirnov and A. Trautner, *GRB 221009A Gamma Rays from Radiative Decay of Heavy Neutrinos?*, *arXiv e-prints* (2022) arXiv:2211.00634 [2211.00634].
- [48] B.T. Zhang, K. Murase, K. Ioka, D. Song, C. Yuan and P. Mészáros, *External Inverse-Compton and Proton Synchrotron Emission from the Reverse Shock as the Origin of VHE Gamma-Rays from the Hyper-Bright GRB 221009A*, *arXiv e-prints* (2022) arXiv:2211.05754 [2211.05754].
- [49] L. Sironi, U. Keshet and M. Lemoine, *Relativistic Shocks: Particle Acceleration and Magnetization*, *Space Sci. Rev.* **191** (2015) 519 [1506.02034].
- [50] S. Das and S. Razzaque, *Ultrahigh-energy cosmic-ray signature in GRB 221009A*, *A&A* **670** (2023) L12 [2210.13349].
- [51] H. Li and B.-Q. Ma, *Lorentz invariance violation induced threshold anomaly versus very-high energy cosmic photon emission from GRB 221009A*, *Astroparticle Physics* **148** (2023) 102831 [2210.06338].
- [52] J.D. Finke and S. Razzaque, *Possible Evidence for Lorentz Invariance Violation in Gamma-Ray Burst 221009A*, *ApJ* **942** (2023) L21 [2210.11261].
- [53] Y.G. Zheng, S.J. Kang, K.R. Zhu, C.Y. Yang and J.M. Bai, *Expected signature for the Lorentz invariance violation effects on γ - γ absorption*, *Phys. Rev. D* **107** (2023) 083001 [2211.01836].
- [54] G. Galanti, M. Roncadelli and F. Tavecchio, *Explanation of the very-high-energy emission from GRB221009A*, *arXiv e-prints* (2022) arXiv:2210.05659 [2210.05659].
- [55] A. Baktash, D. Horns and M. Meyer, *Interpretation of multi-TeV photons from GRB221009A*, *arXiv e-prints* (2022) arXiv:2210.07172 [2210.07172].
- [56] S.V. Troitsky, *Parameters of Axion-Like Particles Required to Explain High-Energy Photons from GRB 221009A*, *Soviet Journal of Experimental and Theoretical Physics Letters* **116** (2022) 767 [2210.09250].
- [57] M.M. González, D. Avila Rojas, A. Pratts, S. Hernández-Cadena, N. Fraija, R. Alfaro et al., *GRB 221009A: A Light Dark Matter Burst or an Extremely Bright Inverse Compton Component?*, *ApJ* **944** (2023) 178 [2210.15857].
- [58] G. Raffelt and L. Stodolsky, *Mixing of the photon with low-mass particles*, *Phys. Rev. D* **37** (1988) 1237.
- [59] A. Mirizzi and D. Montanino, *Stochastic conversions of TeV photons into axion-like particles in extragalactic magnetic fields*, *J. Cosmology Astropart. Phys.* **2009** (2009) 004 [0911.0015].
- [60] A. De Angelis, G. Galanti and M. Roncadelli, *Relevance of axionlike particles for very-high-energy astrophysics*, *Phys. Rev. D* **84** (2011) 105030.
- [61] X. Bi, Y. Gao, J. Guo, N. Houston, T. Li, F. Xu et al., *Axion and dark photon limits from Crab Nebula high-energy gamma rays*, *Phys. Rev. D* **103** (2021) 043018 [2002.01796].
- [62] M. Meyer, J. Davies and J. Kuhlmann, *gammaALPs: An open-source python package for computing photon-axion-like-particle oscillations in astrophysical environments*, in *37th International Cosmic Ray Conference*, p. 557, Mar., 2022, DOI [2108.02061].
- [63] R.C. Gilmore, R.S. Somerville, J.R. Primack and A. Domínguez, *Semi-analytic modelling of the extragalactic background light and consequences for extragalactic gamma-ray spectra*, *MNRAS* **422** (2012) 3189 [1104.0671].
- [64] R. Jansson and G.R. Farrar, *A New Model of the Galactic Magnetic Field*, *ApJ* **757** (2012) 14 [1204.3662].

- [65] A.S. Kozyrev, D.V. Golovin, M.L. Litvak, I.G. Mitrofanov, A.B. Sanin, Mgns/Bepicolombo Team et al., *Improved IPN localization for GRB 221009A (BepiColombo-MGNS light curve), GRB Coordinates Network* **32805** (2022) 1.
- [66] D. Tak, N. Omodei, Z.L. Uhm, J. Racusin, K. Asano and J. McEnery, *Closure Relations of Gamma-Ray Bursts in High Energy Emission*, *ApJ* **883** (2019) 134 [1910.05418].
- [67] S. Woosley and T. Janka, *The physics of core-collapse supernovae*, *Nature Physics* **1** (2005) 147 [astro-ph/0601261].
- [68] J. Hjorth, J. Sollerman, P. Møller, J.P.U. Fynbo, S.E. Woosley, C. Kouveliotou et al., *A very energetic supernova associated with the γ -ray burst of 29 March 2003*, *Nature* **423** (2003) 847 [astro-ph/0306347].
- [69] A. Payez, C. Evoli, T. Fischer, M. Giannotti, A. Mirizzi and A. Ringwald, *Revisiting the SN1987A gamma-ray limit on ultralight axion-like particles*, *J. Cosmology Astropart. Phys.* **2015** (2015) 006 [1410.3747].
- [70] R.Z. Ferreira, M.C.D. Marsh and E. Müller, *Strong supernovae bounds on ALPs from quantum loops*, *J. Cosmology Astropart. Phys.* **2022** (2022) 057 [2205.07896].
- [71] J.W. Brockway, E.D. Carlson and G.G. Raffelt, *SN 1987A gamma-ray limits on the conversion of pseudoscalars*, *Physics Letters B* **383** (1996) 439 [astro-ph/9605197].
- [72] P. Carena and G. Lucente, *Revisiting axion-electron bremsstrahlung emission rates in astrophysical environments*, *Phys. Rev. D* **103** (2021) 123024.
- [73] T. Fischer, P. Carena, B. Fore, M. Giannotti, A. Mirizzi and S. Reddy, *Observable signatures of enhanced axion emission from protoneutron stars*, *Phys. Rev. D* **104** (2021) 103012.
- [74] P. Carena, T. Fischer, M. Giannotti, G. Guo, G. Martínez-Pinedo and A. Mirizzi, *Improved axion emissivity from a supernova via nucleon-nucleon bremsstrahlung*, *J. Cosmology Astropart. Phys.* **2019** (2019) 016 [1906.11844].
- [75] K. Barth, A. Belov, B. Beltran, H. Bräuninger, J.M. Carmona, J.I. Collar et al., *CAST constraints on the axion-electron coupling*, *J. Cosmology Astropart. Phys.* **2013** (2013) 010 [1302.6283].
- [76] R.-Y. Liu, H.-M. Zhang and X.-Y. Wang, *Constraints on Gamma-Ray Burst Models from GRB 221009A: GeV Gamma Rays versus High-energy Neutrinos*, *ApJ* **943** (2023) L2 [2211.14200].
- [77] L. Nava, *High-energy emission from gamma-ray bursts*, *International Journal of Modern Physics D* **27** (2018) 1842003 [1804.01524].
- [78] S. Nakagawa, F. Takahashi, M. Yamada and W. Yin, *Axion dark matter from first-order phase transition, and very high energy photons from GRB 221009A*, *Physics Letters B* **839** (2023) 137824 [2210.10022].